

A demarcation criterion for hydrogen burning of millinovae

IZUMI HACHISU ¹ AND MARIKO KATO ²

¹*Department of Earth Science and Astronomy, College of Arts and Sciences, University of Tokyo, 3-8-1 Komaba, Meguro-ku, Tokyo 153-8902, Japan*

²*Department of Astronomy, Keio University, Hiyoshi, Yokohama 223-8521, Japan*

ABSTRACT

Millinovae are a new class of transient supersoft X-ray sources with no clear signature of mass ejection. They show similar triangle shapes of V/I band light curves with thousand times fainter peaks than typical classical novae. Maccarone et al. regarded the prototype millinova, ASASSN-16oh, as a dwarf nova and interpreted the supersoft X-rays to originate from an accretion belt on a white dwarf (WD). Kato et al. proposed a nova model induced by a high-rate mass-accretion during a dwarf nova outburst; the X-rays originate from the photosphere of a hydrogen-burning hot WD whereas the V/I band photons are from the irradiated accretion disk. Because each peak brightness differs largely from millinova to millinova, we suspect that not all the millinova candidates host a hydrogen burning WD. Based on the light curve analysis of the classical nova KT Eri that has a bright disk, we find that the disk is more than two magnitudes brighter when the disk is irradiated by the hydrogen burning WD than when not irradiated. We present the demarcation criterion for hydrogen burning to be $I_q - I_{\max} > 2.2$, where I_q and I_{\max} are the I magnitudes in quiescence and at maximum light, respectively. Among many candidates, this requirement is satisfied with the two millinovae in which soft X-rays were detected.

Keywords: nova, cataclysmic variables – stars: individual (ASASSN-16oh, KT Eri) – X-rays: binaries

1. INTRODUCTION

A millinova is a transient supersoft X-ray source ($L_X \gtrsim 10^{35}$ erg s⁻¹) with no clear signature of mass ejection. The outburst shape of its optical light curve is almost a symmetric triangle, the peak of which are thousand times fainter than those of typical classical novae. Such a new class of cataclysmic variables were dubbed millinovae by P. Mróz et al. (2024).

A representative example of millinovae is ASASSN-16oh, which is a peculiar transient supersoft X-ray source in the Small Magellanic Cloud (SMC) with no mass ejection signature (T. J. Maccarone et al. 2019). The I light curve of the outburst shows a triangle shape, as plotted in Figure 1. This figure also shows the X-ray count rates observed with the Swift/XRT (0.3–10.0 keV). The peak count rate is converted to

the X-ray luminosity of $L_X \sim 1 \times 10^{37}$ erg s⁻¹ (T. J. Maccarone et al. 2019).

A nova is a thermonuclear runaway event on a mass-accreting white dwarf (WD). We show the optical and X-ray light curves of the Galactic classical nova KT Eri in Figures 1 and 2. Novae usually brighten up by $\Delta V \sim 10$ mag or more in a few or tens days and decline in a few months or years. After hydrogen ignites on the WD, the hydrogen-rich envelope expands to a giant star size and emits strong winds (e.g. M. Kato et al. 2022a, for a recent fully self-consistent nova model). The nova brightness is dominated by free-free emission from optically thin ejecta outside the photosphere (see Figure 2b). Thus, the peak optical brightness depends on the maximum wind mass-loss rate (e.g., I. Hachisu & M. Kato 2006, 2015). Due to strong mass loss, the envelope loses its mass and the photosphere gradually shrinks and the photospheric temperature increases. Eventually the nova enters a supersoft X-ray source (SSS) phase after a large part of the initial envelope mass is lost. The envelope mass decreases further due to nuclear burning

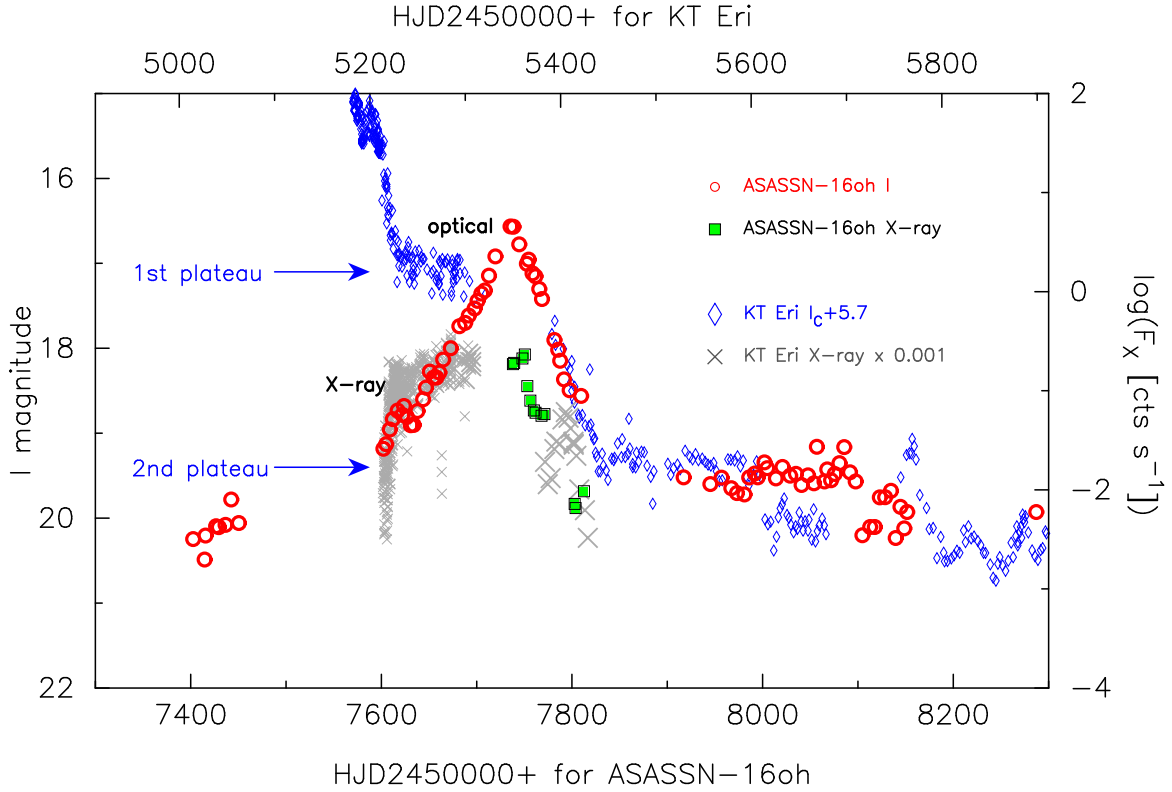


Figure 1. The I light curve of ASASSN-16oh as well as the soft X-ray count rates observed with the Swift/XRT. The data are taken from the OGLE IV (A. Udalski et al. 2015) and the Swift website (P. A. Evans et al. 2009). The I_C and Swift/XRT data of the Galactic classical nova KT Eri are overplotted at the distance of the Small Magellanic Cloud (SMC), the data of which are the same as those in I. Hachisu et al. (2025). The brightnesses of the first and second plateau phases of KT Eri are indicated by the blue arrows.

after the winds stop. Hydrogen burning ends when the envelope mass reaches a critical value. As a definition, a nova accompanies strong winds (mass-ejection) in the optical bright phase. The V/I light curve shapes and peak V/I brightnesses of KT Eri are typical in fast novae and very different from those of millinovae. There seem no common properties between ASASSN-16oh and KT Eri except showing a SSS phase and having a bright disk during the outburst.

A dwarf nova is an rapid accretion event in an accretion disk, the mass accretion of which is temporarily enhanced by a thermal instability of an accretion disk (e.g. Y. Osaki 1996, for a review). If the instability develops from the outer region (outside-in outburst), the brightness rapidly rises toward maximum. On the other hand, when the outburst is inside-out (the instability starts from inside of the disk), the rise is slow and the light curve is more symmetric (triangle) (J.-P. Lasota 2001). Dwarf novae usually brighten up to $M_{V,\text{peak}} \sim +6$ – $+0$ (or by $\Delta V \sim 2$ – 9 mag) in a day or so and stays at the brightness from a few days to a few weeks. The peak brightness depends on the orbital period; the longer the orbital period,

the brighter the $M_{V,\text{peak}}$ (J. Patterson 2011). However, no bright SSS phase ($L_X \gtrsim 1 \times 10^{35}$ erg s $^{-1}$) has ever been observed in dwarf nova outbursts (typically $L_X = 10^{29}$ – 10^{32} erg s $^{-1}$; A. C. Rodriguez et al. 2024; A. D. Schwöpe et al. 2024).

ASASSN-16oh was discovered by the All Sky Automated Survey for Supernovae (ASASSN) at $V = 16.9$ (S. W. Jha et al. 2016). Then, the brightness reaches $M_V = -2.3$, where we assume that the distance modulus is $\mu_0 \equiv (m - M)_0 = 18.9$ and the absorption in the V band is $A_V = 0.13$ toward ASASSN-16oh (S. W. Jha et al. 2016; P. Mróz et al. 2016). The Optical Gravitational Lensing Experiment IV (OGLE-IV) (A. Udalski et al. 2015) data show that the object is an irregular variable for several years with the quiescent luminosity of $I = 20.3$ and $V = 21.1$ (T. J. Maccarone et al. 2019).

The V and I light curves of ASASSN-16oh show a resemblance with those of long orbital-period dwarf novae such as V1017 Sgr in the peak brightness, outburst amplitude, and timescales. The orbital period of V1017 Sgr is $P_{\text{orb}} = 5.786$ days (I. V. Salazar et al. 2017). Therefore, T. J. Maccarone et al. (2019) ex-

pected the orbital period of ASASSN-16oh to be several days. A. Rajoelimanana et al. (2017) reported two peaks (0.1925 and 5.6619 days) in the periodgram of He II λ 4686 spectroscopic velocity data. It is in favor of the longer $P_{\text{orb}} = 5.6619$ days from the resemblance with V1017 Sgr.

It has been argued whether or not soft X-rays in millinova come from a hydrogen burning WD like in the SSS phase of a nova. In the present paper, we find that the classical nova KT Eri is one of the best examples for us to draw such a demarcation line for hydrogen burning in the color-magnitude diagram. In Section 2, we summarize the previous studies on the origin of supersoft X-rays of ASASSN-16oh. In Section 3, we explain physical properties of KT Eri and give the outburst evolution track in the color-magnitude diagram. We also describe the brightness difference between the irradiated disk and viscous heating disk. Section 4 presents the demarcation line in the color-magnitude diagram and apply it to the 29 millinova candidates proposed by P. Mróz et al. (2024). Discussion and conclusions follow in Section 5 and 6, respectively.

2. THE NATURE OF ASASSN-16oh

2.1. Maccarone et al.'s model

T. J. Maccarone et al. (2019) concluded that ASASSN-16oh is an accretion event like a dwarf nova but unlikely a classical nova (thermonuclear runaway event), mainly because (1) the optical spectra show a very narrow width of He II emission lines with no signature of mass-ejection, (2) very slow rise (~ 200 days) to the optical maximum compared with those of classical novae (a few days), (3) rather faint peak V magnitude of $M_{V,\text{max}} \sim -2.3$ compared with those of recurrent novae (e.g., the 1 year recurrence period nova M31N 2008-12a of $M_{V,\text{max}} = -7.2$, M. J. Darnley et al. 2015; M. Henze et al. 2018).

Only the concern is the origin of supersoft X-rays because no bright SSS phase ($L_X \gtrsim 1 \times 10^{35}$ erg s $^{-1}$) has been detected in dwarf nova outbursts. T. J. Maccarone et al. (2019) interpreted that the supersoft X-rays could originate from a spreading layer around the equatorial accretion belt. This model requires a very high mass accretion rate of $\dot{M}_{\text{acc}} \sim 3 \times 10^{-7} M_{\odot} \text{ yr}^{-1}$ (2×10^{19} g s $^{-1}$) on a very massive WD of $1.3 M_{\odot}$ to support high temperatures and fluxes for supersoft X-ray.

The hot spreading layer of the accretion belt has not yet been studied in detail. If a disk around a massive WD with high mass-accretion rates always accompanies a hot spreading layer, such supersoft X-rays could be observed in recurrent novae, that is, in the quies-

cent phase of U Sco ($M_{\text{WD}} \sim 1.37 M_{\odot}$ with $\dot{M}_{\text{acc}} \sim 2.5 \times 10^{-7} M_{\odot} \text{ yr}^{-1}$, I. Hachisu et al. 2000) or RS Oph ($\sim 1.35 M_{\odot}$ with $\sim 2 \times 10^{-7} M_{\odot} \text{ yr}^{-1}$, I. Hachisu et al. 2007), but not yet detected (M. Kato et al. 2020). Because ASASSN-16oh is the first dwarf nova with soft X-ray ($L_X \sim 1 \times 10^{37}$ erg s $^{-1}$) detection, its origin of X-rays is particularly interesting.

2.2. Hillman et al.'s model

Y. Hillman et al. (2019) proposed another interpretation of ASASSN-16oh, a thermonuclear runaway event. Their models are $M_{\text{WD}} = 1.1 M_{\odot}$ WD with the mass accretion rate of $\dot{M}_{\text{acc}} = (3.5 - 5) \times 10^{-7} M_{\odot} \text{ yr}^{-1}$. No mass ejection occurs because the shell flash is very weak. They calculated V/I light curves assuming their V/I photons are emitted from the hot WD surface as well as X-rays. Their V/I light curves show rapid-rise and slow-decline shape, but the decline slopes are 10 times slower than the observed light curves. They did not present the X-ray light curves.

M. Kato et al. (2020) calculated the shell flash models with the same parameters as Hillman et al.'s and confirmed that a hot WD with a surface temperature $T > 400,000$ K does not emit many low energy V/I band photons. M. Kato et al. (2020) obtained the V band light curves that show a good agreement with Hillman et al.'s, and conclude that Y. Hillman et al. (2019) adopted a distance modulus $\mu_V \equiv (m - M)_V = 13.0$ rather than the canonical value of 19.0 mag to the SMC. To summarize, Hillman et al.'s light curve is fainter than ASASSN-16oh by 6 mag and decays 10 times slower.

2.3. Kato et al.'s model

Assuming that X-rays and V/I photons are emitted from different regions as interpreted by T. J. Maccarone et al. (2019), M. Kato et al. (2020) proposed a weak shell flash model in which they attributed the X-ray emission to the nova SSS phase. The main differences from Hillman et al.'s model are: (1) The V/I photons originate from the irradiated accretion disk and companion star because the WD is too hot to emit much V/I photons. (2) The WD mass is much more massive ($1.32 M_{\odot}$) than in Hillman et al.'s model ($1.1 M_{\odot}$) to explain the observed fast decay in the X-ray light curve. (3) The hydrogen shell flash was triggered by a massive mass-inflow during a dwarf nova outburst.

M. Kato et al. (2020) presented an X-ray light curve model of a $1.32 M_{\odot}$ WD (with a low metallicity of $Z = 0.001$) that reproduces the temporal decay of the observed X-rays. They concluded that ASASSN-16oh is a dwarf-nova that triggers a nova (hydrogen-burning)

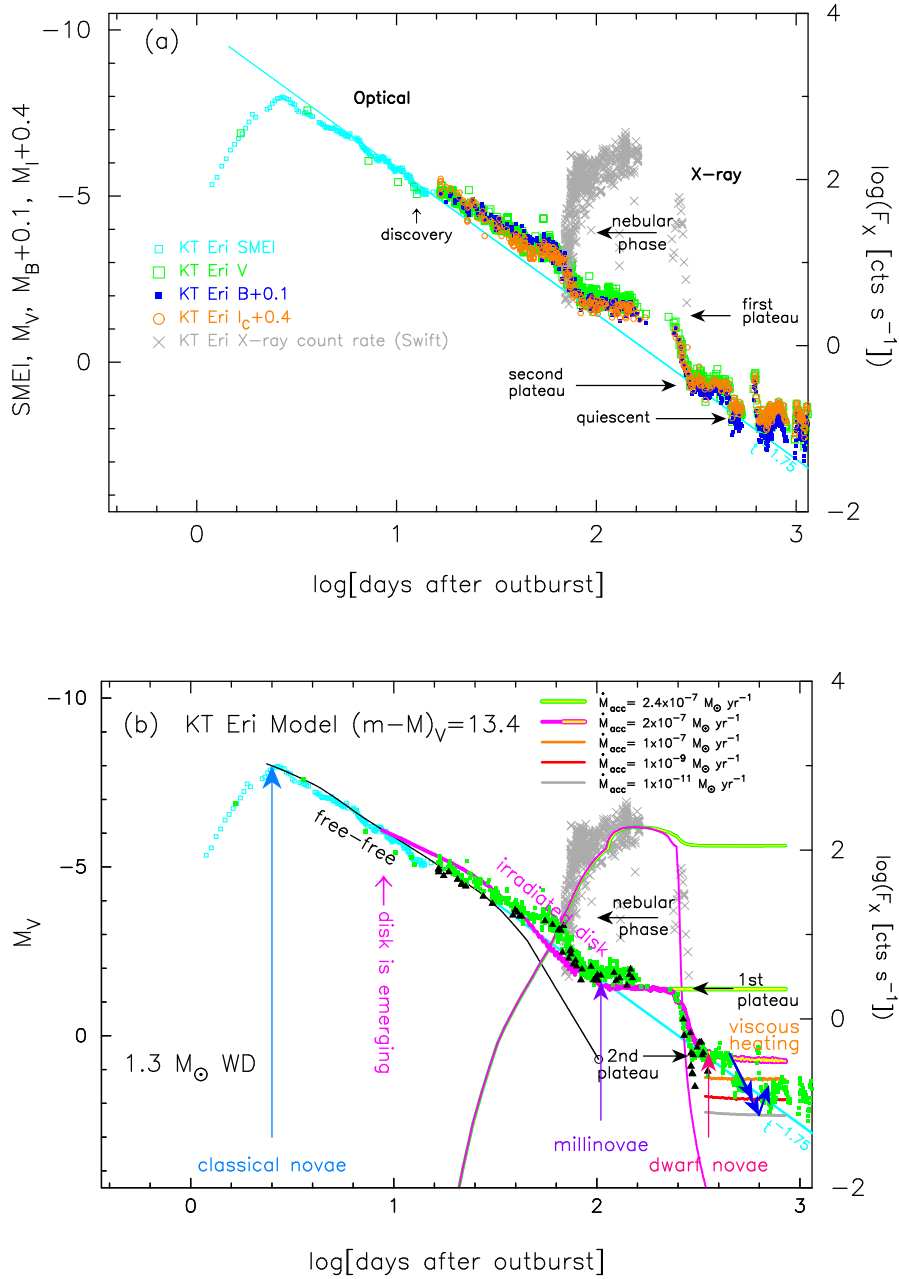


Figure 2. (a) The B, V, I_C , and SMEI magnitudes of KT Eri against a logarithmic time. The B, I_C data are taken from AAVSO, VSOLJ, and SMARTS (F. M. Walter et al. 2012). The outburst day of $t_{\text{OB}} = \text{JD } 2,455,147.5$ is assumed to be 2.7 days before optical (SMEI) maximum. The SMEI, V, y data are the same as those in I. Hachisu et al. (2025). The Swift X-ray (0.3–10.0 keV) count rates are also added (taken from the Swift website; P. A. Evans et al. 2009). The global decay trend is described by the universal decline law of $L_V \propto t^{-1.75}$ (straight cyan line labeled $t^{-1.75}$; I. Hachisu & M. Kato 2006, 2023). The X-ray bright phase (day 68 – 280) is called the supersoft X-ray source (SSS) phase. (b) Our model light curves are overplotted on the SMEI, V , and y (filled black triangles) light curves. The black line denotes the $L_{V,\text{ff,WD}} + L_{V,\text{ph,WD}}$ model light curve while the thick magenta line corresponds to the $L_{V,\text{ff,WD}} + L_{V,\text{ph,WD}} + L_{V,\text{ph,disk}} + L_{V,\text{ph,comp}}$ model light curve for the mass-accretion rate of $\dot{M}_{\text{acc}} = 2 \times 10^{-7} M_{\odot} \text{ yr}^{-1}$. The other thick colored lines represent different mass-accretion rates. See the main text for other symbols. These model light curves are essentially the same as those in I. Hachisu et al. (2025).

with no mass ejection. They further suggested that, in their model, the WD mass increases steadily because of no mass-ejection during the flash, thus, such a massive mass-increasing WD in a low Z environment could be a new kind of candidates for Type Ia supernova progenitors.

2.4. Interpretation on the nature of ASASSN-16oh

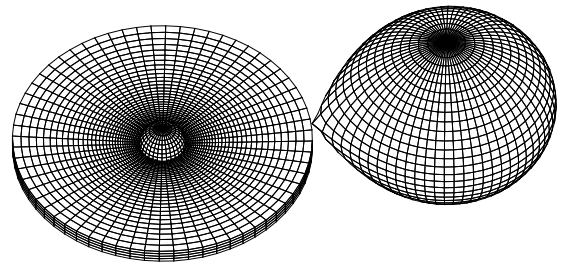
From the above three models, we may conclude that (1) the prototype millinova ASASSN-16oh hosts a massive WD, and (2) its V/I photons mainly come from the (irradiated or viscous heating) accretion disk. (3) The X-rays originate from the surface of hydrogen-burning WD or from the hot accretion belt on the WD. Because the total of 29 millinovae candidates are reported by P. Mróz et al. (2024), it is critically important to find the demarcation line that easily tells us whether or not hydrogen burns on the WD.

3. BRIGHTNESSES OF IRRADIATED DISKS AND VISCOUS HEATING DISKS

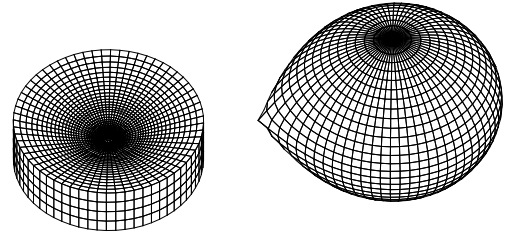
When hydrogen burning starts on the WD, the photospheric temperature becomes high enough to emit super-soft X-ray photons and the luminosity increases closely to the Eddington limit. The photospheric surfaces of the disk and companion star are irradiated by the hot and bright WD. The V/I magnitudes of the irradiated disk and companion star could become much brighter than those of non-irradiated disk and companion star even though the disk itself brightens up with viscous heating.

We found a good example for comparison between irradiated and non-irradiated disk and companion star. Figure 2a shows the optical light curves of the classical nova KT Eri. There are two plateau phases. The first plateau corresponds to the SSS phase, i.e., the WD emits supersoft X-rays. The optical or NIR brightness is governed mainly by the brightness of the accretion disk irradiated by the central hot WD. The absolute I magnitude of the irradiated disk is converted to be about $M_I \sim -2$ at the KT Eri distance modulus of $(m - M)_I = 13.3$ (I. Hachisu et al. 2025). The brightness of the second plateau is explained with the viscous heating disk because hydrogen burning has already ended in this stage (see I. Hachisu et al. 2025, for details).

The viscous-heating disk is two or three magnitudes fainter than the irradiated disk. In the second plateau of KT Eri, I. Hachisu et al. (2025) assumed the mass accretion rate to be as high as $\dot{M}_{\text{acc}} \sim 2 \times 10^{-7} M_{\odot} \text{ yr}^{-1}$, which is close to the steady hydrogen burning rate of $\dot{M}_{\text{acc,steady}} \approx 2.4 \times 10^{-7} M_{\odot} \text{ yr}^{-1}$ for a $1.3 M_{\odot}$ WD. If we assume a lower accretion rate, the brightness of the second plateau becomes fainter as shown in Figure



(a) optically thick wind phase



(b) mass accretion makes a spray

Figure 3. The binary configuration of KT Eri based on the light curve analysis by I. Hachisu et al. (2025). (a) In the wind phase. The disk surface is blown in the winds and its photosphere is slightly expanding. (b) After the wind stops, the disk photosphere shrinks to a normal size. The disk and companion star are irradiated by the supersoft X-ray photons from the central hot WD. Such irradiation effects are all included in the calculation of the V light curve. The masses of the WD and Roche-lobe-filling companion star are $1.3 M_{\odot}$ and $1.0 M_{\odot}$, respectively. The orbital period is $P_{\text{orb}} = 2.616$ days. The inclination angle of the binary is $i = 41.2^{\circ}$. See I. Hachisu & M. Kato (2001) for the calculation methods of V light curves.

2b. If we assume a larger mass accretion rate such as $\dot{M}_{\text{acc}} \gtrsim 2.4 \times 10^{-7} M_{\odot} \text{ yr}^{-1}$ hydrogen burns steadily and never stops. Thus, we may regard that the brightness of the second plateau in KT Eri is close to an upper limit for the brightnesses of viscous heating accretion disks.

In what follows, we first describe the V/I light curves of the classical nova KT Eri and then compare KT Eri with ASASSN-16oh.

3.1. Accretion disk in KT Eri

KT Eri is a fast nova that went into outburst in 2009. Unlike typical classical novae, the orbital period is as long as 2.616 days (B. E. Schaefer et al. 2022). Therefore, it could have a large size accretion disk.

Figure 2a shows the B , V , and I_C light curves of KT Eri. These three light curves almost overlap if we shift down the B and I_C light curves by 0.1 and 0.4 mag,

respectively. This means that the continuum flux dominates the spectra with no significant contribution of emission lines to the BVI_C bands even in the nebular phase. This is not a typical property of classical novae. The optical light curves decay along with the universal decline law of $L_V \propto t^{-1.75}$ (thick cyan line labeled $t^{-1.75}$ in Figure 2a), which is a typical property of classical novae (I. Hachisu & M. Kato 2006, 2023). Here, t is the time from the outburst and L_V is the V band flux.

I. Hachisu et al. (2025) analyzed the B , V , and I_C light curves of KT Eri in detail and calculated V model light curves. They concluded that the first and second plateaus are the manifestation of the bright accretion disk with either irradiation or viscous heating, respectively. Each part is indicated by ‘‘irradiated disk’’ (magenta line) or ‘‘viscous heating’’ (magenta+yellow line) in Figure 2b.

Figure 2b shows the interpretation on the V light curve of KT Eri. The model light curves are calculated by I. Hachisu et al. (2025). They obtained a composite light curve model for a $1.3 M_\odot$ WD, that is, a combination of free-free emission from the nova winds, photospheric luminosities of the WD, and irradiated accretion disk and companion star, that is,

$$L_{V,\text{total}} = L_{V,\text{ff,wind}} + L_{V,\text{ph,WD}} + L_{V,\text{ph,disk}} + L_{V,\text{ph,comp}}, \quad (1)$$

where $L_{V,\text{ph,WD}}$ is the V band flux from the WD photosphere, $L_{V,\text{ph,disk}}$ is the V flux from the optically-thick disk surface (photosphere), $L_{V,\text{ph,comp}}$ the V flux from the companion star photosphere, and $L_{V,\text{ff,wind}}$ is the V flux from free-free emission outside the WD photosphere, which is approximately calculated by

$$L_{V,\text{ff,wind}} = A_{\text{ff}} \frac{\dot{M}_{\text{wind}}^2}{v_{\text{ph}}^2 R_{\text{ph}}}. \quad (2)$$

This $L_{V,\text{ff,wind}}$ represents the flux of free-free emission from optically thin plasma just outside the photosphere, and \dot{M}_{wind} is the wind mass-loss rate, v_{ph} the velocity at the photosphere, and R_{ph} the photospheric radius of the WD. The optically-thick nova winds are accelerated deep inside the photosphere, but the winds become optically thin outside the photosphere. See I. Hachisu et al. (2020) for the derivation of this formula and the coefficient A_{ff} .

The black line labeled free-free denotes the WD components of $L_{V,\text{ff,wind}} + L_{V,\text{ph,WD}}$. In the early phase, the WD photosphere expands to a giant star size and engulfs the companion star. Strong winds blow. Free-free emission from the winds dominates the nova spectrum. Then the WD photosphere gradually shrinks. The irradiation effect of the disk becomes the main optical source after

the disk emerges from the WD photosphere, as shown by the magenta line in Figure 2b. Figure 3 shows our binary configuration after the disk emerges from the WD photosphere.

Around slightly before the optically thick winds ended on day 103, the nova enters the supersoft X-ray source (SSS) phase. There are no bright optical sources except the irradiated accretion disk and companion star, that is, $L_{V,\text{ph,disk}} + L_{V,\text{ph,comp}}$. The model supersoft X-ray light curve is depicted by the thin magenta line in Figure 2b. The X-ray flux (0.3–10.0 keV) is calculated with the blackbody approximation of the WD photosphere.

3.2. Comparison of ASASSN-16oh and KT Eri

Although KT Eri is a classical nova while ASASSN-16oh is a dwarf nova, these two objects show close resemblances. The WD mass of ASASSN-16oh is estimated by M. Kato et al. (2020) to be $1.32 M_\odot$, whereas $1.3 M_\odot$ in KT Eri (I. Hachisu et al. 2025). The orbital period of KT Eri is 2.6 days (B. E. Schaefer et al. 2022) and A. Rajoelimanana et al. (2017) reported 5.66 days for ASASSN-16oh, as mentioned in Section 1.

Figure 1 compares the I light curve of ASASSN-16oh with the I_C light curve of KT Eri at the same distance modulus of SMC. Here we assume that the distance moduli in the I band of ASASSN-16oh and KT Eri are $(m - M)_I = 19.0$ and 13.3 , respectively, i.e., KT Eri is placed 5.7 mag down in the figure. We also shift the time of KT Eri in the horizontal direction to fit its decay of soft X-ray light curve with that of ASASSN-16oh. In this figure, we plot only the middle and late phases of KT Eri because we selectively show the first and second plateau phases of KT Eri.

From the comparison in Figure 1, we are able to list the following points:

1. The duration of the SSS phase of KT Eri is in good agreement with the outburst width of ASASSN-16oh.
2. The brightness of the first plateau of KT Eri is close to, but slightly below, the peak brightness of ASASSN-16oh.
3. The brightness in the second plateau of KT Eri agrees with the brightness in the post-outburst of ASASSN-16oh.
4. The I magnitude decline of KT Eri from the first plateau to the second plateau is well overlapped to that of ASASSN-16oh. This suggests that the cooling timescales both of the WDs are almost the same after hydrogen burning ends.

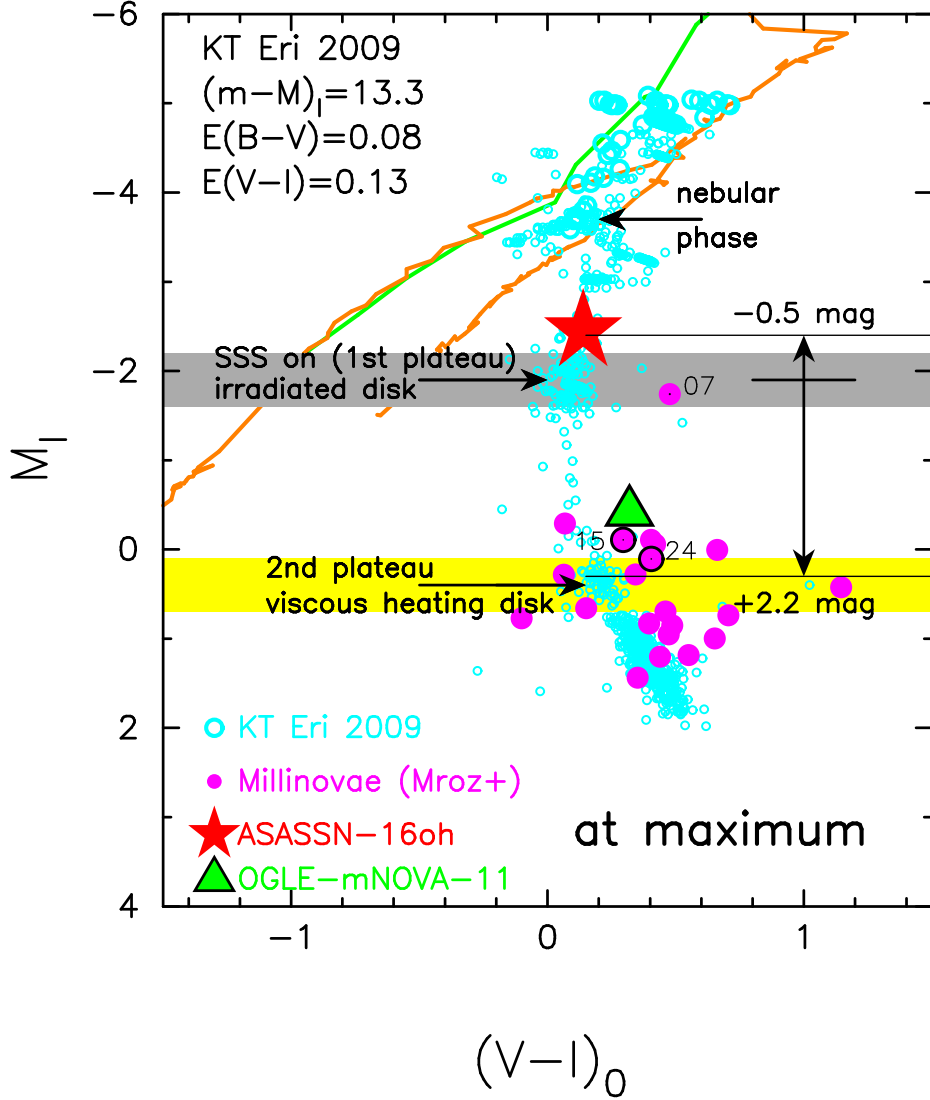


Figure 4. The $(V-I)_0$ - M_I color-magnitude diagram track of KT Eri (open cyan circles) and 23 millinova candidates (among the total 29 millinova candidates) at the outburst peak (filled magenta circles; P. Mróz et al. 2024). Various time epochs of outburst evolution are shown for KT Eri, but only each peak position is depicted for the 23 millinovae (P. Mróz et al. 2024). The filled red star is the peak position of ASASSN-16oh while the filled green triangle is the peak of OGLE-mNOVA-11, both of which are detected in X-ray ($\gtrsim 1 \times 10^{35}$ erg s $^{-1}$). The millinova labeled “07” (encircled “15” and “24”) corresponds to OGLE-mNOVA-07 (-15 and -24) in Table 1 of P. Mróz et al. (2024). The two tracks of V1500 Cyg (thick green line) and LV Vul (thick orange line) are added, taken from Figure 12(b) of I. Hachisu et al. (2025). The horizontal broad gray belt shows the brightnesses in the first plateau (SSS) phase while the yellow belt corresponds to the brightnesses in the second plateau (viscous heating) phase of KT Eri. The effect of inclination angle of binaries are added by the two arrows labeled “-0.5 mag” and “+2.2 mag.” See the main text for more details.

5. The brightness in quiescence of KT Eri ($I_C \sim 14.54 \rightarrow M_I \sim 1.24$) broadly agrees with the brightness in quiescence of ASASSN-16oh ($I \sim 20.27 \rightarrow M_I \sim 1.27$).

These provide important clues to understand the nature of millinovae.

Both the first and second plateaus in KT Eri are explained with/without irradiation by the central WD (I. Hachisu et al. 2025). The peak brightness of

ASASSN-16oh, similar to the KT Eri first plateau, is consistent with that (1) hydrogen burning occurs on the WD and (2) the irradiated disk has a disk surface area similar to KT Eri. It is supported from the suggestion that both the binary systems have similar large orbital periods (a few to several days).

The brightness of the second plateau in the KT Eri is determined by the mass-accretion rate through the disk to the WD because hydrogen burning already ended.

We expect a similar accretion rate to KT Eri in the post-outburst phase of ASASSN-16oh, during at least 300 days, from HJD 2,457,800 to HJD 2,458,100.

Similar cooling timescales of I light curves in KT Eri and ASASSN-16oh indicate the similar (almost the same) WD masses, because the cooling timescale depends strongly on the WD mass. I. Hachisu et al. (2025) estimated the WD mass to be $1.3 M_{\odot}$ for KT Eri while M. Kato et al. (2020) suggested $1.32 M_{\odot}$ for ASASSN-16oh. These two WD mass estimates are consistent with each other. Thus, if ASASSN-16oh hosts a hydrogen burning WD, we may conclude that nuclear burning extinguished soon after the optical peak. Then, the decay from the peak to post-outburst in the V/I light curves indicates the weakening irradiation effect by the cooling WD.

4. DEMARCATION CRITERION FOR HYDROGEN BURNING

4.1. Peak I brightnesses of millinovae

ASASSN-16oh shows a large outburst amplitude of $\Delta I \equiv I_{\text{q}} - I_{\text{max}} = 3.7$ mag, where I_{q} is the mean I magnitude in quiescence and I_{max} the peak I magnitude of the outburst (see Table 1 of P. Mróz et al. 2024). Because the orbital period of ASASSN-16oh is as long as 5.66 days (A. Rajoelimanana et al. 2017), its companion star has already evolved to a subgiant and its mass transfer rate could be much larger than those in typical dwarf novae. ASASSN-16oh could host a large accretion disk around the WD. Thus, dwarf nova outbursts of ASASSN-16oh could be much brighter than typical dwarf novae if the disk is irradiated by the hydrogen burning hot WD.

P. Mróz et al. (2024) found 29 millinovae candidates and summarized various physical quantities including the peak I_{max} brightness and its color $(V - I)_{\text{max}}$. We plot their 23 millinovae (among the total 29 millinovae) in the $(V - I)_0 - M_I$ color-magnitude diagram in Figure 4 together with the evolution track of KT Eri. ASASSN-16oh is indicated by the large filled red star mark.

KT Eri evolves downward and stays at the first plateau of $M_I \sim -1.9 \pm 0.3$ during the SSS phase. Here, ± 0.3 mag represents scatters in the I_{C} magnitude distribution during the first plateau (see Figures 4 and 5). Its brightness can be reproduced by an accretion disk irradiated by the hydrogen burning hot WD, as shown in Figure 2b with a model of Figure 3b. The peak I magnitude of ASASSN-16oh is located slightly above the first plateau of KT Eri, as in Figure 4. We therefore may conclude that, if ASASSN-16oh hosts a hydrogen-burning WD, its peak I brightness can be explained by an accretion disk irradiated by this hot WD.

Thus, we define the demarcation line for hydrogen-burning to be $M_{I,1} = -1.9 \pm 0.3$ (horizontal gray belt zone).

Next, we set another demarcation line, $M_{I,2} = 0.3 \pm 0.3$ (horizontal yellow belt zone). This corresponds to the I brightness of the second plateau of KT Eri. Because the hydrogen burning has already ended, the I brightness in the second plateau can be explained by viscous heating in the accretion disk. The brightness depends mainly on the mass-accretion rate. I. Hachisu et al. (2025) reproduced the V brightness in the second plateau of KT Eri by assuming the mass-accretion rate of $\dot{M}_{\text{acc}} = 2 \times 10^{-7} M_{\odot} \text{ yr}^{-1}$. It should be noted again that this rate is close to the lower bound for steady hydrogen burning, and could give an upper bound for the brightness of viscous heating. If the mass accretion rate is larger than $\dot{M}_{\text{acc}} \approx 2.4 \times 10^{-7} M_{\odot} \text{ yr}^{-1}$, hydrogen burns steadily (as shown in Figure 2b) and the V brightness keeps $M_{V,1} \sim -1.8$, much brighter than the V brightness in the second plateau, $M_{V,2} \sim +0.5$.

In Figure 4, many millinova candidates are located ~ 2 mag below the position of ASASSN-16oh, and close to or on the yellow belt line. Moreover, its distribution is scattered with a width of more than 2 mag. This suggests that no hydrogen burning occurs in some fainter objects and some candidates brighten up only by viscous heating.

4.2. Dependence on the binary inclination

The brightness of the disk depends on the inclination angle i of a binary (e.g., $i = 41.2^\circ$ for KT Eri: I. Hachisu et al. 2025). For dwarf novae at or near maximum light, the surface of the accretion disk can be assumed to be optically thick, and in this case, B. Paczyński & A. Schwarzenberg-Czerny (1980) found that, for a binary with the inclination angle of i , the magnitude of a flat, limb-darkened (with $u = 0.6$) disk should be corrected by

$$\Delta M_I(i) = -2.5 \log\left[\left(1 + \frac{3}{2} \cos i\right) \cos i\right] + 2.5 \log\left[\left(1 + \frac{3}{2} \cos 41.2^\circ\right) \cos 41.2^\circ\right]. \quad (3)$$

This shows a strong dependence on the inclination angle: a pole-on disk is about 0.5 mag brighter than KT Eri, while stars with deep eclipses (typically $i > 80^\circ$) should be at least 2.2 mag fainter than that of KT Eri.

The demarcation line moves up and down if we include the effect of the inclination, especially, toward a high inclination binary. We suppose that supersoft X-rays are originated from a hydrogen burning WD. If a soft X-ray flux of $L_X \gtrsim 1 \times 10^{35} \text{ erg s}^{-1}$ is detected from a millinova, it indicates that hydrogen burns on

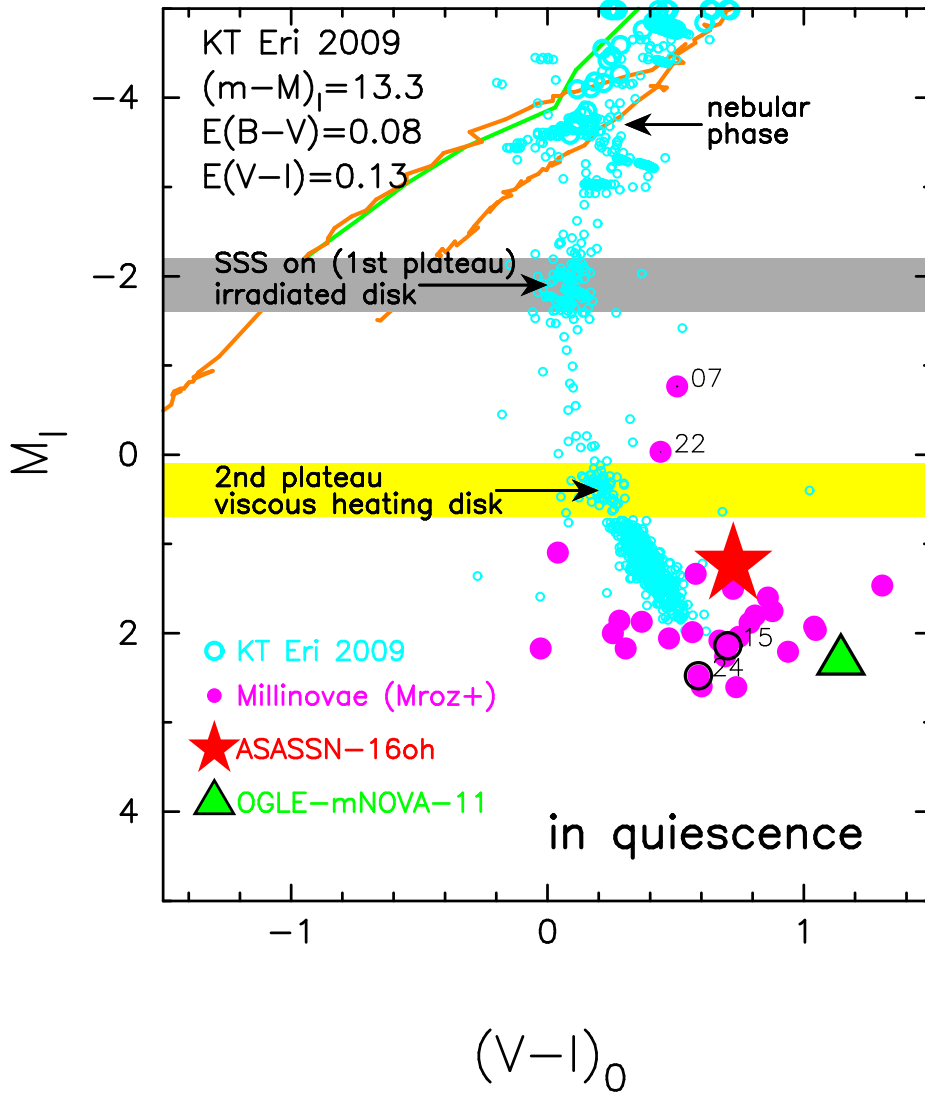


Figure 5. Same as Figure 4, but for quiescent phases of the 29 millinova candidates. The two millinovae labeled “07” and “22” corresponds to OGLE-mNOVA-07 and OGLE-mNOVA-22 (P. Mróz et al. 2024), respectively. The two millinovae of 07 and 22 are brighter than the yellow belt (the second plateau of KT Eri) and could not be the members of the SMC or LMC.

the surface of the WD even if its optical peak is ~ 2 mag fainter than the gray belt demarcation line (first plateau of KT Eri), as shown in Figure 4. For a low inclination angle (view from near pole-on), on the other hand, its optical peak could be ~ 0.5 mag brighter than the gray belt demarcation line. This covers the position of ASASSN-16oh.

To summarize, for a transient supersoft X-ray source (millinova) with $L_X \gtrsim 1 \times 10^{35}$ erg s $^{-1}$ or so, we regard that hydrogen burns on the surface of the WD when it is brighter than $M_{I,1,\text{faint}} \equiv M_{I,1} + 2.2 = -1.9 + 2.2 = 0.3$ mag. If no X-rays are detected and fainter than $M_{I,\text{peak}} \gtrsim M_{I,2} = +0.3$, we suppose that this object belongs to normal dwarf novae. The large scatter of millinova $M_{I,\text{peak}}$ in Figure 4 may reflect the scatter in the inclination angle.

If our interpretation is correct, there is a trend that the fainter the $M_{I,\text{peak}}$, the smaller the supersoft X-ray flux L_X . This is because the photosphere of the WD is more shielded by the disk edge for a higher inclination binary.

It is interesting that the peak position of OGLE-mNOVA-11 (filled green triangle) is upper than $M_{I,1,\text{faint}} = +0.3$ mag (thin horizontal black line labeled “+2.2 mag” in Figure 4). An X-ray flux of $L_X \sim 1 \times 10^{35}$ erg s $^{-1}$ is detected. We may conclude that hydrogen burns on the WD but a large part of the WD photosphere is occulted by a flaring-up disk edge or something else (see, e.g., discussion of Y. Hillman et al. 2019).

4.3. Quiescent brightnesses of millinovae

Figure 5 shows the positions of 29 millinovae candidates in quiescence (P. Mróz et al. 2024). Many of them are located below the second plateau (yellow belt line) in the $(V - I)_0 - M_I$ color-magnitude diagram and their brightnesses are consistent with the quiescent brightness of KT Eri. This indicates that, in quiescence, the mass-accretion rate is substantially lower than $\dot{M}_{\text{acc}} = 2 \times 10^{-7} M_{\odot} \text{ yr}^{-1}$ unless the inclination angle is as high as $i \gtrsim 75^\circ$.

There are two millinovae above the second plateau of KT Eri. These two millinovae labeled “07” and “22” correspond to OGLE-mNOVA-07 and OGLE-mNOVA-22 (P. Mróz et al. 2024), respectively. If these two millinovae shine by viscous heating in the accretion disk, their mass-accretion rates should be much higher than $\dot{M}_{\text{acc}} = 2 \times 10^{-7} M_{\odot} \text{ yr}^{-1}$. With such a high mass-accretion rate, hydrogen burning is stable as shown in Figure 2b, and the disk should be irradiated all the time. In this case, we expect a constant brightness of $M_{I,1} = -1.9$ (or $M_{V,1} = -1.8$, yellow+orange line in Figure 2b). Therefore, we may conclude that these two millinovae candidates are not millinovae, but much fainter dwarf novae in our Galaxy (foreground stars). The rise in the brightness from quiescence to maximum is $\Delta I \equiv I_q - I_{\text{max}} = 0.98$ in OGLE-mNOVA-07 and $\Delta I \equiv I_q - I_{\text{max}} = 0.92$ in OGLE-mNOVA-22, being much smaller than the other millinovae, for example, $\Delta I = I_q - I_{\text{max}} = 3.68$ in ASASSN-16oh (OGLE-mNOVA-01) and $\Delta I = I_q - I_{\text{max}} = 2.73$ in OGLE-mNOVA-11. Thus, the yellow belt demarcation line can be utilized to distinguish millinovae from typical foreground dwarf novae.

In this way, we utilize our demarcation line of the second plateau (viscous heating) to distinguish millinovae in the SMC and LMC from foreground dwarf novae in our Galaxy.

4.4. Amplitudes of the millinova outbursts

Millinovae stay below the second plateau line of $M_{I,2} = +0.3$ because the mass accretion rate is smaller than $\dot{M}_{\text{acc}} \sim 2 \times 10^{-7} M_{\odot} \text{ yr}^{-1}$. If they go into outburst by triggering thermal instability of a disk and hydrogen burns on the WDs, their brightnesses reach at least $M_{I,2} = -1.9$ like in KT Eri because of irradiation effect. Thus, their amplitudes of outburst should exceed

$$\Delta I \equiv I_q - I_{\text{max}} \gtrsim M_{I,2} - M_{I,1} = 2.2. \quad (4)$$

The amplitude of ASASSN-16oh, $\Delta I = I_q - I_{\text{max}} = 3.7$, satisfies this requirement (see ΔI in Table 1 of P. Mróz et al. 2024). OGLE-mNOVA-11 also has the amplitude of $\Delta I = I_q - I_{\text{max}} = 2.7$ and the X-ray fluxes of $L_X \sim 1 \times 10^{35} \text{ erg s}^{-1}$ were detected. We

conclude that hydrogen burns on the WD for mNOVA-11. Two millinova candidates show marginal amplitudes of $\Delta I = I_q - I_{\text{max}} = 2.2$ (mNOVA-15) and 2.4 (mNOVA-24). If an X-ray flux of $L_X \gtrsim 1 \times 10^{35} \text{ erg s}^{-1}$ is observed, we conclude that hydrogen burns in these millinovae (encircled magenta symbols labeled “15” and “24” in Figures 4 and 5).

A millinova candidate of $\Delta I = I_q - I_{\text{max}} \lesssim 2$ is unlikely to host a hydrogen burning WD. We do not expect bright X-ray fluxes of $L_X \gtrsim 1 \times 10^{35} \text{ erg s}^{-1}$. Therefore, it is not a millinova by definition.

In this way, the outburst amplitude can be used to find a millinova. If the amplitude of an outburst satisfies $\Delta I = I_q - I_{\text{max}} \gtrsim 2.2$ (Equation (4)) and the peak I magnitude is brighter than $M_{I,1,\text{faint}} = +0.3 \text{ mag}$, it is possibly a millinova and an X-ray flux of $L_X \gtrsim 1 \times 10^{35} \text{ erg s}^{-1}$ would be detected. Note that the requirement of Equation (4) is independent of the inclination angle i of the binary.

5. DISCUSSION

5.1. A Dwarf Nova Triggers a Nova Outburst?

M. Kato et al. (2020) discussed the possibility that a dwarf nova outburst can trigger a nova outburst. They showed that an accreting WD experiences a nova outburst when the mass of the hydrogen-rich envelope reaches a critical value (see, e.g., Table 1 of M. Kato et al. 2020). The critical masses are a few to several times $10^{-7} M_{\odot}$ for the case of ASASSN-16oh, that is, for a $1.32 M_{\odot}$ WD with the heavy element content of $Z = 0.001$ (or $1.35 M_{\odot}$ WD and $Z = 0.0001$). This low metallicity corresponds to a typical metallicity of the SMC ($[\text{Fe}/\text{H}] = -1.25 \pm 0.01$) (M.-R. L. Cioni 2009). In general, the ignition mass is smaller for a larger mass-accretion rate of \dot{M}_{acc} (or a shorter recurrence period of t_{rec}) because the WD is hotter.

It is useful to see how the hydrogen-rich envelope decreases its mass with time in KT Eri. The envelope mass was $M_{\text{env,max}} = 2.9 \times 10^{-6} M_{\odot}$ at optical maximum, and decreases to $M_{\text{env,ws}} = 3.2 \times 10^{-7} M_{\odot}$ when winds stop. Thus, for a hydrogen shell flash on a similar WD mass, wind mass loss occurs when the ignition mass is larger than $M_{\text{env,ws}} = 3.2 \times 10^{-7} M_{\odot}$. The envelope mass in KT Eri further decreases to $M_{\text{env,hb}} = 1.9 \times 10^{-7} M_{\odot}$ when the hydrogen burning stops. This means that, if the ignition mass is between $3.2 \times 10^{-7} M_{\odot}$ and $1.9 \times 10^{-7} M_{\odot}$, the nuclear burning ignites on the WD with no mass ejection. This broadly fit with the definition of millinova. If the hydrogen-rich envelope mass is smaller than $1.9 \times 10^{-7} M_{\odot}$, hydrogen never ignites.

Thus, we can divide a thermonuclear runaway event by the amount of the ignition mass into a classical nova,

millinova, and dwarf nova (no runaway). The corresponding brightnesses are roughly indicated with the upward arrows labeled “classical novae”, “millinovae”, and “dwarf novae” in Figure 2b.

The mass-accretion rate onto the WD is estimated in several dwarf novae by [M. Kimura et al. \(2018\)](#). Among them, V364 Lib shows a relatively large mass inflow rate of $1 \times 10^{-7} M_{\odot} \text{ yr}^{-1}$. This object has an orbital period of $P_{\text{orb}} = 0.70$ days, rising (decay) time of 10 (35) days, and small outburst amplitude of 1 mag. If we apply this mass-accretion rate to KT Eri, the total accreted mass reaches $((10 + 35)/365) \times (1 \times 10^{-7} M_{\odot} \text{ yr}^{-1}) = 1.2 \times 10^{-8} M_{\odot}$ at most during the outburst, being too small to ignite hydrogen on the WD.

In the case of ASASSN-16oh, we expect a much larger mass inflow rate as suggested from a much larger outburst amplitude ($\Delta I = I_{\text{q}} - I_{\text{max}} = 3.68$) and longer orbital period (5.66 days, [A. Rajoelimanana et al. 2017](#)). If we assume the mass inflow rate of several times $10^{-7} M_{\odot} \text{ yr}^{-1}$, the WD may accrete sufficient mass for hydrogen ignition, that is, $(200/365) \times (5 \times 10^{-7} M_{\odot} \text{ yr}^{-1}) = 2.7 \times 10^{-7} M_{\odot}$ before maximum (see Figure 1). This is between $3.2 \times 10^{-7} M_{\odot}$ and $1.9 \times 10^{-7} M_{\odot}$, and satisfies the condition of millinova.

5.2. The brightness of the first plateau

The brightnesses of the first and second plateau, $M_{I,1}$ and $M_{I,2}$ could depend not only on the inclination angle i but also on the other binary parameters. In this subsection, we discuss the dependence of the first plateau brightness ($M_{V,1}$ or $M_{I,1}$) on the WD mass, metallicity, and orbital period.

5.2.1. white dwarf mass and metallicity

The WD luminosity in the SSS phase is estimated to be close to the Eddington luminosity (e.g., [M. Kato et al. 2022b](#)),

$$L_{\text{ph}} \approx L_{\text{Edd}} \equiv \frac{4\pi c G M_{\text{WD}}}{\kappa_{\text{el}}}, \quad (5)$$

where L_{ph} is the photospheric luminosity of the WD, c the speed of light, G the gravitational constant, M_{WD} the mass of the WD, and κ_{el} the electron scattering opacity. The irradiation effect is mainly determined by the luminosity of the central WD and therefore the brightness of $M_{V,1}$ or $M_{I,1}$ depends approximately on $M_{\text{WD}}/\kappa_{\text{el}}$. In the SSS phase, the photospheric temperature of the WD is as high as $\sim 10^6$ K and hydrogen and helium atoms are completely ionized at the photosphere. Then, the opacity is expressed by $\kappa_{\text{ph}} \approx \kappa_{\text{el}} = 0.2(1+X) \text{ cm}^{-2} \text{ g}^{-1}$, where κ_{ph} is the opacity at the photosphere and X is the hydrogen content (by mass weight). Thus,

Table 1. Brightnesses of the first and second plateau phases^a

P_{orb}	$M_{V,1}$	$M_{V,2}$	$M_{I,1}$	$M_{I,2}$
(day)	(mag)	(mag)	(mag)	(mag)
5.66	-2.4	0.0	-2.5	-0.2
2.62	-1.8	0.5	-1.9	0.3
1.23	-1.1	1.2	-1.2	1.0

^a $M_{\text{WD}} = 1.3 M_{\odot}$; $M_2 = 1.0 M_{\odot}$; $T_{\text{ph},2} = 4500$ K; the inclination angle of the binary $i = 41.2^\circ$; $M_{\text{acc}} = 2 \times 10^{-7} M_{\odot} \text{ yr}^{-1}$; P_{orb} is the orbital period of the binary; $M_{V,1}/M_{I,1}$ the absolute V/I brightnesses at the first plateau; $M_{V,2}/M_{I,2}$ the absolute V/I brightnesses at the second plateau.

the metallicity difference between LMC/SMC and our Galaxy does not make a significant difference in the brightness of $M_{V,1}$ or $M_{I,1}$.

The WD mass can be restricted from the condition that mass accretion by single dwarf nova outburst triggers nuclear burning on the WD. We estimate the amount of mass supplied by the dwarf nova instability in ASASSN-16oh to be as small as several times $10^{-7} M_{\odot}$ (see Section 5.1). This value may correspond to the largest accreted mass for millinovae because ASASSN-16oh is the brightest one among the 29 millinovae candidates ([P. Mróz et al. 2024](#)).

The ignition mass is defined by the mass of a hydrogen-rich envelope when thermonuclear runaway starts on a WD, and is presented for various WD masses and mass accretion rates in Figure 2 of [M. Kato et al. \(2021\)](#). The ignition mass depends on the mass accretion rate, but the ignition mass of several times $10^{-7} M_{\odot}$ appears only on the WD mass of $M_{\text{WD}} > 1.3 M_{\odot}$. A less massive WD ($M_{\text{WD}} < 1.3 M_{\odot}$) needs repeated dwarf nova outbursts before the envelope mass reaches the required ignition mass. In this case, however, hydrogen burning lasts much longer than the case of ASASSN-16oh (e.g., for a $1.2 M_{\odot}$ WD, its duration is 10 times longer, see [Y. Hillman et al. 2019](#); [M. Kato et al. 2020](#)). Thus, we can exclude WD masses of $M_{\text{WD}} < 1.3 M_{\odot}$ if a millinova hosts a hydrogen burning WD.

The brightness of the first plateau depends linearly on the WD mass (see Equation (5)). Because a hydrogen burning millinova hosts a very massive WD, the brightness difference by the WD mass is smaller than 5%, that is, 0.1 mag in the $M_{V,1}$ or $M_{I,1}$.

5.2.2. orbital period

The brightnesses at the first and second plateaus depend on the orbital period P_{orb} of the binary because a large P_{orb} binary could have a large accretion disk. We have calculated the V light curves using the KT Eri model but for two different orbital periods of 5.66 days (ASASSN-16oh) and 1.23 days (U Sco). Table 1 shows the brightnesses of $M_{V,1}$, $M_{V,2}$, $M_{I,1}$, and $M_{I,2}$ for these orbital periods including the $P_{\text{orb}} = 2.62$ days of KT Eri. The other binary parameters are assumed to be the same as those in KT Eri. For $P_{\text{orb}} = 5.66$ days, $\Delta M_{V,1} = -0.6$ mag brighter, but for $P_{\text{orb}} = 1.23$ days, $\Delta M_{V,1} = +0.7$ mag fainter than in KT Eri.

It is important that the brightness difference between the first plateau and the second plateau is still $M_{V,2} - M_{V,1} = 2.2$ or 2.3 and $M_{I,2} - M_{I,1} = 2.2$ or 2.3 among the three P_{orb} cases. Therefore, our requirement of $I_{\text{q}} - I_{\text{max}} \gtrsim 2.2$ mag (Equation (4) in Section 4.4) is safely satisfied. The peak I brightness of ASASSN-16oh is $M_{I,\text{max}} = -2.4$ (the inclination angle i is not known) and consistent with our result of $M_{I,1} = -2.5$ ($i = 41.2^\circ$ in KT Eri) in Table 1.

P. Mróz et al. (2024) suggested the decay timescales (τ_{d}) of millinovae are between $20 \lesssim \tau_{\text{d}} \lesssim 70$ days mag^{-1} and this range corresponds roughly to $3 \lesssim P_{\text{orb}} \lesssim 16$ days from the relation in their Figure 6. Only two millinovae have known orbital periods of 5.66 days (ASASSN-16oh) and 4.83 days (OGLE-mNOVA-08). We suppose that ASASSN-16oh has the longest orbital period because it is the brightest one among the 29 millinova candidates. On the other hand, KT Eri has the orbital period of 2.62 days, which corresponds possibly to the shortest case. Therefore, the range of $M_{I,1}$ is between -2.5 and -1.9 for typical millinovae if they have a hydrogen burning WD.

5.3. A possible way to Type Ia supernovae?

It should be noted that there is an essential difference between millinovae and classical novae: a millinova has no mass ejection during the outburst while a classical nova loses almost all accreted mass by winds. In other words, the mass retention efficiency is about 100% in millinovae. Because the WD mass of ASASSN-16oh is already as massive as $1.32 M_{\odot}$, M. Kato et al. (2020) suggested that ASASSN-16oh is a candidate of Type Ia supernova progenitors. When the WD mass reaches $1.38 M_{\odot}$, it could explode as a Type Ia supernova. In this sense, millinovae are also promising objects for Type Ia supernova progenitors.

6. CONCLUSIONS

Our main results are summarized as follows.

1. We define the demarcation criterion of millinovae for hydrogen burning, that is, $M_{I,1} = -1.9 \pm 0.3$, based on the first plateau of the KT Eri 2009 outburst.
2. ASASSN-16oh satisfies the above demarcation criterion for hydrogen burning. Also at optical maximum, its position is just on the KT Eri track of the 2009 outburst in the $(V - I)_0 - M_I$ color-magnitude diagram. This confirms that the brightness of ASASSN-16oh is dominated by an irradiated accretion disk.
3. We also find another demarcation criterion for an upper limit for viscous heating disks, $M_{I,2} = 0.3 \pm 0.3$, based on the second plateau of the KT Eri 2009 outburst. Millinova candidates, the peak magnitudes of which are fainter than $M_{I,2}$, are highly likely to be a dwarf nova, but not a millinova.
4. There are two millinova candidates substantially above $M_{I,2}$ in quiescence, i.e., OGLE-mNOVA-07 and OGLE-mNOVA-22. If they were really the members of the LMC, hydrogen should burn steadily on the WD in quiescence. Therefore, we may conclude that these two millinova candidates are not millinovae but much fainter foreground dwarf novae (in our Galaxy). In this way, we utilize our second demarcation line of $M_{I,2}$ to distinguish millinovae (nuclear burning object) in the SMC/LMC from foreground dwarf novae (viscous heating) in our Galaxy.
5. The brightnesses of demarcation lines depend on the inclination angle i of the disk (or binary). The dependency on the angle i is given by Equation (3). A pole-on disk is about 0.5 mag brighter than that of KT Eri ($i = 41.2^\circ$), while stars with deep eclipses (typically $i > 80^\circ$) are ~ 2.2 mag fainter than KT Eri.
6. To trigger hydrogen burning on a WD by only one dwarf nova instability, its ignition mass should be as small as $\sim 1 \times 10^{-6} M_{\odot}$ or less, which requires the WD mass of $M_{\text{WD}} \gtrsim 1.3 M_{\odot}$.
7. Among the 29 millinova candidates, ASASSN-16oh ($P_{\text{orb}} = 5.66$ days) is the brightest at maximum and possibly has the longest orbital period. On the other hand, KT Eri has the orbital period of 2.62 days, which corresponds to the shortest one, possibly the faintest one. Therefore, the

range of the first plateau brightness $M_{I,1}$ is between -2.5 and -1.9 for typical millinovae if they have a hydrogen burning WD.

8. When the amplitude of an outburst satisfies $\Delta I \equiv I_q - I_{\max} \gtrsim 2.2$ (Equation (4)), a detection of soft X-ray flux $L_X \gtrsim 1 \times 10^{35}$ erg s $^{-1}$ supports this argument of an irradiated accretion disk. The two millinovae, ASASSN-16oh ($\Delta I = 3.7$) and OGLE-mNOVA-11 ($\Delta I = 2.7$), satisfy these requirements. The first requirement of $\Delta I \gtrsim 2.2$ is independent either of the inclination angle or of the orbital period of the binary. We find two more millinovae that marginally satisfy this requirement, OGLE-mNOVA-15 ($\Delta I = 2.2$) and OGLE-mNOVA-24 ($\Delta I = 2.4$).
9. We predict a tendency; for a fainter I_{\max} millinova, a smaller X-ray flux is observed.

10. For a millinova candidate having a small amplitude of $\Delta I = I_q - I_{\max} \lesssim 2$, it is unlikely that it hosts a hydrogen burning white dwarf (WD). It is not a millinova by definition. We do not expect bright X-ray fluxes of $L_X \gtrsim 1 \times 10^{35}$ erg s $^{-1}$.
11. Because the mass retention efficiency is about 100% in millinova outbursts and its WD mass is already as massive as $\gtrsim 1.3 M_{\odot}$, the WD soon reaches $1.38 M_{\odot}$ and could explode as a Type Ia supernova. Therefore, millinovae are promising candidates for Type Ia supernova progenitors.

We are grateful to the Variable Star Observers League of Japan (VSOLJ) and the American Association of Variable Star Observers (AAVSO) for the archive data of KT Eri. We also thank the anonymous referee for useful comments that improved the manuscript.

Facilities: Swift(XRT), AAVSO, SMARTS, VSOLJ, OGLE IV

REFERENCES

- Cioni, M.-R. L. 2009, A&A, 506, 1137, <https://doi.org/10.1051/0004-6361/200912138>
- Darnley, M. J., Henze, M., Steele, I. A., et al. 2015, A&A, 580, A45, <https://doi.org/10.1051/0004-6361/201526027>
- Evans, P. A., Beardmore, A. P., Page, K. L., et al. 2009, MNRAS, 397, 1177, <https://doi.org/10.1111/j.1365-2966.2009.14913.x>
- Hachisu, I., & Kato, M. 2001, ApJ, 558, 323, <https://doi.org/10.1086/321601>
- Hachisu, I., & Kato, M. 2006, ApJS, 167, 59, <https://doi.org/10.1086/508063>
- Hachisu, I., & Kato, M. 2015, ApJ, 798, 76, <https://doi.org/10.1088/0004-637X/798/2/76>
- Hachisu, I., & Kato, M. 2021, ApJS, 253, 27, <https://doi.org/10.3847/1538-4365/abd31e>
- Hachisu, I., & Kato, M. 2023, ApJ, 953, 78, <https://doi.org/10.3847/1538-4357/acdfd3>
- Hachisu, I., Kato, M., Kato, T., & Matsumoto, K. 2000, ApJL, 528, L97, <https://doi.org/10.1086/312684>
- Hachisu, I., Kato, M., & Luna, G. J. M. 2007, ApJL, 659, L153, <https://doi.org/10.1086/516838>
- Hachisu, I., Kato, M., & Walter, F. 2025, ApJ, 980, 142, <https://doi.org/10.3847/1538-4357/adae08>
- Hachisu, I., Saio, H., Kato, M., Henze, M., & Shafter, A. W. 2020, ApJ, 902, 91, <https://doi.org/10.3847/1538-4357/abb5fa>
- Henze, M., Darnley, M. J., Williams, S. C., et al. 2018, ApJ, 857, 68, <https://doi.org/10.3847/1538-4357/aab6a6>
- Hillman, Y., Orio, M., Prialnik, D., et al. 2019, ApJL, 879, L5, <https://doi.org/10.3847/2041-8213/ab2887>
- Hounsell, R., Bode, M. F., Hick, P. P., et al. 2010, ApJ, 724, 480, <https://doi.org/10.1088/0004-637X/724/1/480>
- Jha, S. W., Colmenero, E. R., Stanek, K. Z., et al. 2016, The Astronomer's Telegram, 9859, 1
- Kato, M. 1999, PASJ, 51, 525, <https://doi.org/10.1093/pasj/51.4.525>
- Kato, M., Saio, H., & Hachisu, I. 2020, ApJ, 892, 15, <https://doi.org/10.3847/1538-4357/ab7996>
- Kato, M., Saio, H., & Hachisu, I. 2021, PASJ, 73, 1137, <https://doi.org/10.1093/pasj/psab0764>
- Kato, M., Saio, H., & Hachisu, I. 2022a, PASJ, 74, 1005, <https://doi.org/10.1093/pasj/psac051>
- Kato, M., Saio, H., & Hachisu, I. 2022b, ApJL, 935, L15, <https://doi.org/10.3847/2041-8213/ac85c1>
- Kimura, M., Kato, T., Maehara, H., et al. 2018, PASJ, 709, 78, <https://doi.org/10.1093/pasj/psy073>
- Lasota, J.-P. 2001, New Astronomy Reviews, 45, 449, [https://doi.org/10.1016/S1387-6473\(01\)00112-9](https://doi.org/10.1016/S1387-6473(01)00112-9)
- Maccarone, T. J., Nelson, T. J., Brown, P. J., et al. 2019, Nature Astronomy, 3, 173, <https://doi.org/10.1038/s41550-018-0639-1>

- Mróz, P., Udalski, A., Wyrzykowski, L., Kozłowski, S., & Poleski, R. 2016, *The Astronomer's Telegram*, 9867, 1
- Mróz, P., Król, K., Szegedi, K., et al. 2024, *ApJL*, 977, L37, <https://doi.org/10.3847/2041-8213/ad969b>
- Osaki, Y. 1996, *PASP*, 108, 39, <https://doi.org/10.1086/133689>
- Paczyński, B., & Schwarzenberg-Czerny, A. 1980, *Acta Astronomica*, 30, 127
- Patterson, J. 2011, *MNRAS*, 411, 2695, <https://doi.org/10.1111/j.1365-2966.2010.17881.x>
- Ragan, E., Brozek, T., Suchomska, K., et al. 2009, *ATel*, 2327, 1
- Rajoelimanana, A., Charles, P., Buckley, D., & Meintjes, P. 2017, in *5th Annual Conference on High Energy Astrophysics in Southern Africa*, eds. P. Meintjes et al., (SISSA: Trieste, Italy), 319, 3, <https://doi.org/10.22323/1.319.0003>
- Rodriguez, A. C., El-Badry, K., Suleimanov, V., et al. 2024, arXiv:2408.16053
- Salazar, I. V., LeBleu, A., Schaefer, B. E., Landolt, A. U., & Dvorak, S. 2017, *MNRAS*, 469, 4116, <https://doi.org/10.1093/mnras/stx1161>
- Schaefer, B. E., Walter, F. M., Hounsell, R., Hillman, Y. 2022, *MNRAS*, 517, 3864, <https://doi.org/10.1093/mnras/stac2923>
- Schwöpe, A. D., Knauff, K., Kurpas, J., et al. 2024, *A&A*, 690, A243, <https://doi.org/10.1051/0004-6361/202450537>
- Udalski, A., Szymański, M.K., Szymański, G. 2015, *Acta Astronomica*, 65, 1
- Walter, F. M., Battisti, A., Towers, S. E., Bond, H. E., & Stringfellow, G. S. 2012, *PASP*, 124, 1057, <https://doi.org/10.1086/668404>